Apoptosis (2022) 27:409–425
https://doi.org/10.1007/s10495-022-01725-0

Inhibition of miR-130b-3p restores autophagy and attenuates intervertebral disc degeneration through mediating ATG14 and PRKAA1

Tongde Wu[1] · Xuebing Jia[2] · Ziqi Zhu[1] · Kai Guo[1] · Qiang Wang[1] · Zhiqiang Gao[1] · Xinhua Li[3] · Yufeng Huang[1] · Desheng Wu[1]

Accepted: 15 March 2022 / Published online: 18 April 2022

Abstract

Oxidative stress-induced autophagy dysfunction is involved in the pathogenesis of intervertebral disc degeneration (IVDD). MicroRNAs (miRNAs) not only have been regarded as important regulators of IVDD but also reported to be related to autophagy. This research was aimed to explore the role of miR-130b-3p in IVDD and its regulation on autophagy mechanism. The miR-130b-3p expression in the patient's degenerative nucleus pulposus (NP) samples and rat NP tissues was detected by qRT-PCR and FISH assay. The miR-130b-3p was knocked down or overexpressed in the human NP cells by lentivirus transfection. TBHP was used to induce oxidative stress in the human NP cells. Apoptosis, senescence, and autophagy were evaluated by flow cytometry, β-gal staining, immunofluorescence, electron microscopy, and Western blot in the miR-130b-3p knocked down human NP cells under TBHP treatment. The relationship between the miR-130b-3p and ATG14 or PRKAA1 was confirmed by luciferase assay. The siRNA transfection was used to knock down the ATG14 and PRKAA1 expression, and then the human NP cells functions were further determined. In the in vivo experiment, the IVDD rat model was constructed and an adeno-associated virus (AAV)-miR-130b-3p inhibitor was intradiscally injected. After that, MRI and histological staining were conducted to evaluate the role of miR-130b-3p inhibition in the IVDD rat model. We found that the miR-130b-3p was upregulated in the degenerative NP samples from humans and rats. Interestingly, the inhibition of miR-130b-3p rescued oxidative stress-induced dysfunction of the human NP cells, and miR-130b-3p inhibition upregulated autophagy. Mechanistically, we confirmed that the miR-130b-3p regulated the ATG14 and PRKAA1 directly and the knockdown of the ATG14 or PRKAA1 as well as the treatment of autophagy inhibitor blockaded the autophagic flux and reversed the protective effects of miR-130b-3p inhibition in the TBHP-induced human NP cells. Furthermore, the inhibition of the miR-130b-3p via AAV- miR-130b-3p injection ameliorated the IVDD in a rat model. These data demonstrated that the miR-130b-3p inhibition could upregulate the autophagic flux and alleviate the IVDD via targeting ATG14 and PRKAA1. The translational potential of this article: The suppression of miR-130b-3p may become an effective therapeutic strategy for IVDD.

Keywords Intervertebral disc degeneration · Autophagy · miR-130b-3p · Nucleus pulposus · Oxidative stress

Tongde Wua, Xuebing Jiab, Ziqi Zhua and Kai Guo have contributed equally to this work.

✉ Yufeng Huang
surgeonhng@alumni.tongji.edu.cn

✉ Desheng Wu
eastspinewudesheng@126.com

[1] Department of Spine Surgery, Shanghai East Hospital, Pudong District, Tongji University School of Medicine, 150 Jimo Rd, Shanghai 200120, China

[2] Cancer Center, Shanghai General Hospital, Shanghai Jiao Tong University School of Medicine, Shanghai 200080, China

[3] Department of Orthopedics, Shanghai General Hospital, Shanghai Jiao Tong University School of Medicine, Shanghai 200080, China

Introduction

It is reported that about 84% of the general population experienced low back pain (LBP) at some point in their span of life [1]. The LBP is the leading cause of disability worldwide, which causes a huge economic burden both to the patients and society [2]. Intervertebral disc degeneration (IVDD) is the main etiological factor of the LBP and other degenerative disc diseases [3]. The intervertebral disc mainly consists of the inner nucleus pulposus (NP) and surrounding annulus fibrosus. The NP cells are centrally located in the NP. In the process of the IVDD, the NP cells dysfunction, produce excessive extracellular matrix (ECM) enzymes, and decrease the expression of ECM-related proteins such as collagen II and aggrecan, indicating the imbalance between the anabolic and catabolic activities [4, 5]. Previous studies have reported that oxidative stress was involved in the apoptosis, senescence, and aberrant ECM metabolism of the NP cells in the IVDD [6, 7]. Many factors such as aging, smoking, spinal trauma, and genetics could promote oxidative stress in the NP cells [8, 9]. However, the pathogenetic mechanism of IVDD is still vague and effective therapies are urged to be found.

Autophagy is a fundamental cellular process through which cells digest dysfunctional organelles and proteins to produce necessary substances for their survival and function [10]. Previous studies have found that autophagy was related to many diseases, such as osteoarthritis, Alzheimer's disease, and diabetic cardiomyopathy [11–13]. Furthermore, the constitutive autophagy of the NP cells played a protective role against oxidative stress [10, 14, 15]. But the mechanism of the protection is still unknown.

MicroRNAs (miRNAs) are a class of endogenous, single-stranded, and noncoding RNAs that negatively regulate the target gene expression post-transcriptionally via binding to the 3′-untranslated regions (3′-UTRs) of the complementary mRNAs [16]. Accumulating evidence supports that the miRNAs play a critical role in the proliferation, apoptosis, and autophagy of multiple cells. Several studies have reported that some miRNAs were involved in the IVDD. For example, miR-141 promoted the IVDD development by targeting the SIRT1/NF-κB pathway and miR-200c inhibition alleviated the inflammatory cytokines induced by the NP cell apoptosis [3, 4]. In particular, miR-21, miR-210, miR-96-5p, and miR-101-3p have been reported to be involved in regulating autophagy in the human NP cells [17–19]. However, whether the miRNAs could regulate the oxidative stress-induced dysfunction of the NP cells through autophagy in the IVDD, was rarely investigated.

Among miRNAs, miR-130b has been reported to function as an oncogene in various cancers [20]. In addition, previous studies reported that the inhibition of miR-130b-3p exerted a protective effect on the placental trophoblast cells against oxidative stress [21]. In our study, we found that miR-130b-3p was dysregulated in degenerative NP tissues and miR-130b-3p played a significant role in the process of IVDD both in vivo and vitro. Mechanistically, we revealed that miR-130b-3p could regulate autophagy through targeting ATG14 and PRKAA1. The ATG14, also known as beclin-1-associated autophagy-related key regulator (Barkor or ATG14L), exerted its function in enhancing the membrane tethering and fusion of autophagosomes to endolysosomes during autophagy while the PRKAA1 (protein kinase AMP-activated catalytic subunit alpha 1) was reported to involve in multiple diseases, including leukemia, wound healing, and osteoarthritis via autophagy [22–25]. Our research demonstrated that miR-130b-3p inhibition could upregulate the autophagic flux and alleviate the IVDD via targeting ATG14 and PRKAA1. Collectively, the suppression of the miR-130b-3p may become an effective therapeutic strategy for IVDD.

Materials and methods

NP tissue specimens

Forty-five degenerative NP tissues were collected from the patients with lumbar disc degeneration. Fourteen rat NP tissues were isolated from the normal rats and the model rats of the IVDD. These fresh NP samples were placed in the RNAlater solution (Invitrogen Corp., Carlsbad, CA, USA) at 4 ℃ overnight and then stored at − 80 °C. As our previous study described, the human degenerative intervertebral disc samples were divided into four categories (II, III, IV, and V) according to the Pfirrmann grading system [26, 27]. The detailed information of the patient intervertebral disc samples is summarized in Supplemental Table 1.

The RNA extraction and quantitative reverse transcription-PCR (qRT-PCR)

The total RNAs from the NP tissues or the NP cells were extracted using the miRNeasy Mini Kit (Qiagen, Valencia, CA, USA). To determine the miRNA levels in the NP tissues or NP cells, the RNA was reverse-transcribed using Mir-X miRNA First-Strand Synthesis Kit (Takara, Kusatsu, Japan). The cDNA was used as a template to perform qRT-PCR using a QuantiTect SYBR Green PCR Kit (Takara) in an Applied Biosystems 7500 System. The comparative Ct (ΔΔCt) method was used to analyze the relative fold changes of the miRNA. The U6 was used as the endogenous control for the miRNA normalization. All primers are shown in Supplemental Table 2.

Human NP cells lentivirus and siRNA transfection

Human NP cells were purchased from ScienCell Research Lab. Inc. (Carlsbad, CA, USA) and cultured in the human NP cell medium (ScienCell) as previously described [28]. The oxidative stress in the cells was induced by Tert-butyl hydro-peroxide (TBHP; Sigma-Aldrich, St. Louis, MO, USA) for 24 h. Stable transfectants overexpressing miR-130b-3p(PGMLV-CMV-hsa-miR-130b-3p-PGK-Puro,LV-miR-130b-3p), knocking down miR-130b-3p (hsa-miR-130b-3p inhibitor), and the negative control were constructed using the lentiviral transfer vector (Genomeditech, Shanghai, China) at a multiplicity of infection (MOI) of 60. The lentivirus infection was performed when the NP cells reached 40–60% confluency. The miR-130b-3p expression was detected by the quantitative reverse transcription-PCR (qRT-PCR) to evaluate the transfection efficiency. To suppress the expression of ATG14 and PRKAA1, the NP cells at 70–80% confluency were transfected with the ATG14 siRNA, PRKAA1 siRNA, and control scrambled siRNA (Genomeditech) according to the manufacturer's protocol. The Western blot was used to assess the transfection efficiency. The target sequences of the ATG14 siRNA and PRKAA1 siRNA are shown in Supplemental Table 2.

RNA fluorescent in situ hybridization (FISH)

The FISH assay was used to detect the miR-130b-3p level in the human degenerative NP samples (Pfirrmann grades II and Pfirrmann grades V). The digoxin-labeled miR-130b-3p probes with locked nucleic acid modification were used in the FISH (Exonbio, Guangzhou, China). The sequence of the miR-130b-3p probes is shown in Supplemental Table 2. As previously described the NP samples sections were deparaffinized and rehydrated before the incubation with the hybridization mixture [3]. The signals of the digoxin-labeled miR-130b-3p probes were detected using tyramide-conjugated Cy3 and 4,6-diamidino-2-phenylindole (DAPI, Invitrogen) was used to counterstain the cell nucleus.

Western blot analysis

The total protein from the human NP cells or tissues were lysed in RIPA buffer containing protease and phosphatase inhibitors. The protein concentrations were measured by the BCA protein assay kit (Beyotime, Haimen, China). And the protein samples were electrophoresed on SDS-PAGE gel and transferred to PVDF membranes (Millipore Corp., Burlington, MA, USA). After blocking with 5% skim milk in TBST for 1 h, the membranes were incubated with primary antibody at 4 °C overnight. These primary antibodies include Caspase-3 (1:1000, Cell Signaling Technology (CST)), Caspase-7 (1:1000, CST), Caspase-9 (1:1000, CST), p16 INK4A (1:1000, CST), ATG14 (1:1000, CST), LC3A/B (1:1000, CST), Beclin-1 (1:1000, CST), SQSTM1/p62 (1:1000, CST), PRKAA1 (1:1000, Abcam), aggrecan (1:1000, Abcam), collagen II (1:1000, Abcam), MMP13 (1:3000, Abcam), ADAMTS4 (1:1000, Abcam), and GAPDH (1:2500, Abcam). The membranes were then incubated with the HRP-linked anti-mouse or anti-rabbit IgG (1:1000, CST) at room temperature for 1 h. The Immunoblots were detected using the ECL solution (Invitrogen) and measured using the ImageJ software (National Institutes of Health, MD, USA).

Flow cytometry analysis

The human NP cell apoptotic rates were detected using an Annexin V/PI apoptosis detection kit (BD Biosciences, Franklin Lakes, NJ, USA). After washing twice with the cold PBS, the cells were resuspended in a binding buffer and incubated with 5 μL FITC-Annexin V and 10 μL PI in the dark at room temperature for 20 min. The apoptotic cells were analyzed using the FACScan flow cytometry system (Becton Dickinson, San Diego, CA, USA).

SA-β-gal staining

The SA-β-gal staining kit (Beyotime) was used to detect the level of senescence of the human NP cells. Briefly, the cells were fixed at room temperature for 15 min and then incubated with the X-gal working solution at 37 °C overnight. The aged NP cells were stained blue. The images were captured using a general optical microscope (Leica, Wetzlar, Germany).

Immunofluorescence

As previously described, the human NP cells were fixed in 4% paraformaldehyde, incubated with 0.1% Triton X-100 for 25 min, and then blocked with 5% BSA containing 0.1% Triton X-100 for 30 min at RT [29]. Subsequently, the cells were incubated with the primary antibodies against MMP13 (1:200, Abcam) and collagen II (1:200, Abcam) at 4 °C overnight and the relevant secondary antibodies for 1 h in the dark, and then counterstained with the DAPI for another 5 min. The fluorescence was visualized using a fluorescence microscope (Leica DMI3000B, Leica Microsystems Inc.).

Autophagic flux analysis

The human NP cells at 60% confluency were infected with the AdV-mRFP-GFP-LC3 (MOI = 300; Hanbio, Shanghai, China) according to the manufacturer's instructions. After the NP cells were infected for 8 h, the culture medium was changed. And the fluorescence was observed using a fluorescence microscope after 48 h of transfection (Leica

DMI3000B, Leica Microsystems Inc.). As described previously, the autophagy flux was evaluated, the yellow dot indicated the merge fluorescence of both GFP (green) and RFP (red), which represented an autophagosome, while autolysosomes were viewed as red dots in the merged images [30]. The number of dots per cell was counted in the original images. The 3-Methyladenine (3-MA: 10 mM, Sigma-Aldrich) was used to block the autophagy in the human NP cells.

Electron microscopy

The human NP cells were fixed in 2.5% glutaraldehyde overnight, post-fixed in 2% osmium tetroxide, and stained with 2% uranyl acetate. After the dehydration in acetone, the human NP cells were cut into semi-thin sections (Leica EM UC7 ultramicrotome) and followed by toluidine blue staining. Images were obtained using a transmission electron microscope (Tecnai G2 Spirit, FEI, Hillsboro, OR, USA).

Luciferase reporter assay

The miR-130b-3p target genes ATG14 and PRKAA1 were predicted by TargetScan (http://www.targetscan.org/) webserver. The wild-type 3'UTR and mutant 3'UTR of the ATG14 and PRKAA1 were inserted into the pmirGLO luciferase vector (Promega Corp., Madison, WI, USA). According to the manufacture's recommendations, the HEK 293 cells were co-transfected with 100 ng reporter plasmid and 30 nM miR-130b-3p mimics or control using Opti-MEM media (Invitrogen) and Lipofectamine 3000 transfection reagent. The corresponding primers are shown in Supplemental Table 2. After 48 h, the luciferase activity was detected using the Dual-Luciferase Reporter Assay System (Promega Corp). The activity of Renilla luciferase was used to normalize the firefly luciferase activity.

Construction of the IVDD rat model and the intradiscal injection of miR-130b-3p inhibitor

Adult male Sprague–Dawley (SD, SPF and weighing 250–300 g) were purchased from the Shanghai Slac Laboratory Animal Co. Ltd. The rats were randomly divided into four groups (Control, IVDD, miR-130b-3p inhibitor, and Inhibitor control). The IVDD rat model was constructed as previously described [26]. In brief, the rats were anesthetized by intraperitoneal injection of 5% chloral hydrate (6 mL/kg) and the Co7/8 of the vertebral discs were vertically punctured using a 21-gauge needle from the AF to the NP (depth: 5 mm). After the puncture, the needle was rotated 180° and held for 30 s. Subsequently, a total of 3 μL HBAAV2/9-rno-Mir-130b-3p-sponge-EGFP or HBAAV2/9-EGFP NC (Hanbio biotechnology Shanghai Co., Ltd.) was slowly injected into the punctured discs using a 27-gauge needle (Hamilton, Bonaduz, Switzerland) and a microliter syringe. The sequences of primers are shown in Supplemental Table 2. After the operation, the rats were returned to their cages and monitored daily to ensure their health condition.

MRI examination

To assess the effect of the miR-130b-3p inhibitor on the IVDD rats, the MRI examination was carried out at 0 weeks, 4 weeks, and 8 weeks after the surgery using a 3.0 T MRI system (Philips Eclipse, Aachen, Germany). The specific parameters of MRI scanning were referred to in the previous study [31]. The rat vertebral disc signal intensity of the sagittal T2-weighted images was evaluated by the two blinded researchers and the rat intervertebral disc degeneration grades were classified based on the Pfirrmann classification [27].

Histological and immunofluorescent staining of the tissue sections

All rat intervertebral disc samples were obtained from the Co7/8 and fixed in 4% paraformaldehyde. After decalcification using EDTA solution, the disc samples were embedded in paraffin and cut into Sects. (5 μm). Hematoxylin–eosin (HE) and Safranin O-Fast green (SO) staining were carried out to evaluate the histological scores of the rat intervertebral discs based on a modified histologic grading system [4]. For immunofluorescent staining, the section was deparaffinized and incubated in the antigen retrieval solution. The primary antibodies used were as follows: EGFP (1:100, Abcam), LC3A/B (1:100, CST), ATG14 (1:200, CST), PRKAA1 (1:250, Abcam), and collagen II (1:200, Abcam). After the incubation with the corresponding secondary antibodies, the sections were then counterstained with the DAPI. The fluorescence was visualized using a fluorescence microscope (Leica).

Statistical analysis

All data were presented as mean ± S.D. The statistical analyses were performed using GraphPad Prism 7 Software (San Diego, CA, USA). The student's t-tests were performed to analyze the statistical significance between the two groups. Multiple groups were analyzed by one-way analysis of variance (ANOVA) followed by Tukey's test for the comparison between the two groups. The correlation between the miR-130b-3p expression and the Pfirrmann grade of the human degenerative intervertebral disc was determined by the Spearman's rank correlation coefficient. The $P < 0.05$ was considered significant.

Result

The upregulation of the miR-130b-3p in the degenerative NP samples from humans and rats

First, we detected the miR-130b-3p level in the human degenerative NP tissues obtained from 45 patients, 23 patients with lumbar disc herniation, and 22 patients with lumbar spinal stenosis (see Supplemental Table 1 for details of the patients). The NP tissues were classified into 4 groups (Pfirrmann grades II, III, IV, and V) according to the T2-weighted MRI images (Fig. 1A). The miR-130b-3p expression was significantly upregulated in the IVDD patients with the Pfirrmann grades IV and V when compared with the Pfirrmann grades II and III patients, which was further validated by fluorescence in situ hybridization (Fish) assay (Fig. 1B, D, $P = 0.0003$). Furthermore, the miR-130b-3p expression was positively correlated with the Pfirrmann grades of the IVDD patients ($n = 45$, $r = 0.619$) (Fig. 1C, $P < 0.001$). We also determined the miR-130b-3p level in the IVDD rat model. The IVDD model was successfully constructed through the needle puncture, which presented lower T2-weighted signal intensities in the MRI image (Fig. 1E). Consistently, the qRT-PCR results also indicated that the miR-130b-3p level was increased in the degenerative rat NP tissues (Fig. 1F, $P = 0.0021$). These data indicated that the miR-130b-3p may play a crucial role in the process of IVDD.

Inhibition of the miR-130b-3p rescues the oxidative stress-induced dysfunction of human NP cells

To further investigate the biological function of the miR-130b-3p in the IVDD, stably overexpressed and knocked down miR-130b-3p in the human NP cells were successfully established through the lentivirus infection (Fig. 2A, $P < 0.05$). Oxidative stress is a critical risk condition in the development of IVDD. In our study, the TBHP (100 μM) was used to induce oxidative stress in the human NP cells. Firstly, we found that the TBHP treatment increased the miR-130b-3p expression in the human NP cells, which was blocked by the miR-130b-3p inhibition (Fig. 2B, $P < 0.05$). Subsequently, we explored the effects of the miR-130b-3p knockdown on apoptosis, senescence, and degeneration-associated proteins expression in the human NP cells. The Western blot and flow cytometry results indicated that the miR-130b-3p knockdown not only suppressed the apoptotic protein level but also decreased the apoptosis percentage of the cells stimulated by the TBHP treatment (Fig. 2C–E, $P < 0.001$). Compared with the control group, the percentage of SA-β-gal-positive cells in the TBHP treatment group, was increased, whereas the miR-130b-3p inhibition reduced the percentage of the senescent cells under the condition of oxidative stress (Fig. 2F–H, $P < 0.01$). Furthermore, as shown in Fig. 2I–K, the TBHP remarkably suppressed collagen II and aggrecan expression but stimulated the expression of MMP13 and ADAMTS4. Interestingly, the miR-130b-3p knockdown promoted the collagen II and aggrecan synthesis as well as suppressed the expression of catabolic enzymes. Collectively, these results demonstrated that the inhibition of the miR-130b-3p could protect the human NP cells from oxidative stress-induced dysfunction.

The miR-130b-3p inhibition upregulates the autophagy in the human NP cells under oxidative stress

Previous studies have reported that the autophagy impairment induced by oxidative stress was involved in the IVDD [32]. Therefore, whether the miR-130b-3p could regulate autophagy in the IVDD or not was explored in our study. Firstly, electron microscopy (TEM) was used to detect the autophagic vesicles. We found that the inhibition of the miR-130b-3p could upregulate the number of autophagosomes and autolysosomes compared with the inhibitor control group, in which the autophagy was inhibited by the TBHP stimulation. And 3-methyladenine (3-MA), an autophagy inhibitor significantly blocked the autophagy (Fig. 3A). Subsequently, to further observe the autophagy flux, the mRFP-GFP-LC3 adenovirus (AdV-mRFP-GFP-LC3) was transfected into the human NP cells. The autolysosomes were red puncta because the GFP was quenched in the acidic environment of the lysosomes and the autophagosomes produced both mRFP and GFP signals labeled in yellow. This system provided us with an effective way to determine the autophagic flux. As shown in Fig. 3B, C, after the TBHP stimulation, in contrast to the control group, both mRFP and GFP signals were reduced in the TBHP group ($P < 0.05$). However, a remarkable rise in the number of both autophagosomes and autolysosomes was found in the miR-130b-3p inhibitor group ($P < 0.01$). Meanwhile, when the 3-MA was added, the changes of the autophagic flux were canceled ($P < 0.01$). Furthermore, the autophagy-related proteins were detected via the Western Blot. Compared with the untreated controls, protein levels of LC3-II, Beclin-1, and P62 were not significantly changed after the TBHP treatment ($P > 0.05$). Intriguingly, both LC3-II/LC3-I ratio and Beclin-1levels are considerably increased by the miR-130b-3p inhibition while P62 level was decreased ($P < 0.05$). Consistently, the 3-MA could reverse all autophagy-related proteins changes [Fig. 3D–F, ($P < 0.01$)]. These data suggested that the inhibition of miR-130b-3p could upregulate autophagy,

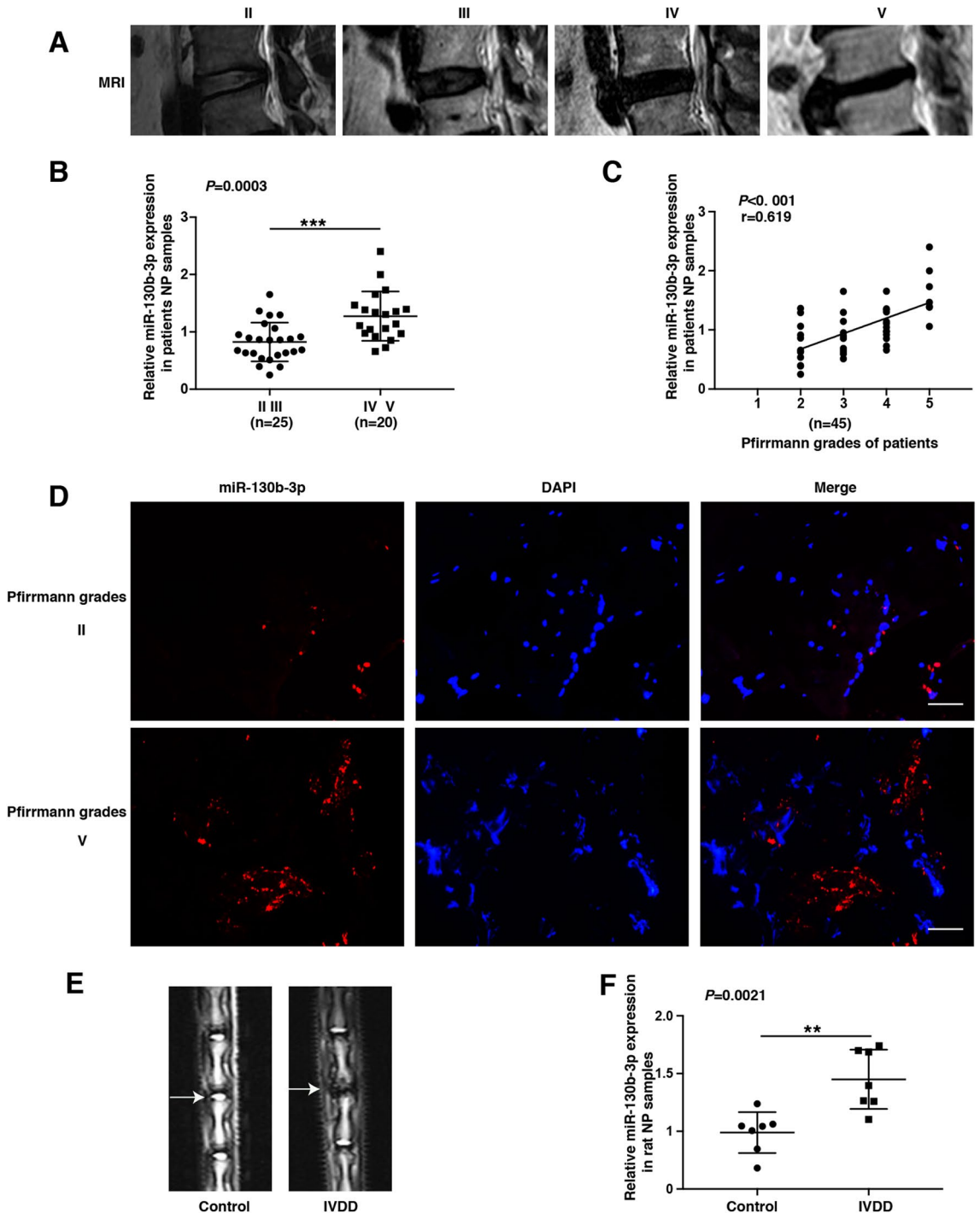

Fig. 1 The miR-130b-3p was upregulated in degenerative NP samples of humans and rats. **A** The representative T2-weighted MRI images for the different Pfirrmann grades (II, III, IV, and V). **B** miR-130b-3p expression was higher in grades IV and V of the NP tissues (n = 20) than in grades II and III (n = 25) ($P < 0.001$). **C** The level of miR-130b-3p in NP tissues from IVDD patients was positively correlated with the disc degeneration grades (n = 45, r = 0.619, and $P < 0.001$). **D** FISH assay of the NP tissues from IVDD patients indicated the increased level of miR-130b-3p in severe degenerative NP tissue compared with mild ones. (Scale bar = 25 μm). **E** MRI images of control and IVDD groups of rats. **F** Quantitative analysis of the level of miR-130b-3p in the control and degenerated rat discs (n = 7). All data is presented as the mean ± SD. MRI: magnetic resonance imaging. IVDD: intervertebral disc degeneration. *$P < 0.05$; **$P < 0.01$; ***$P < 0.001$

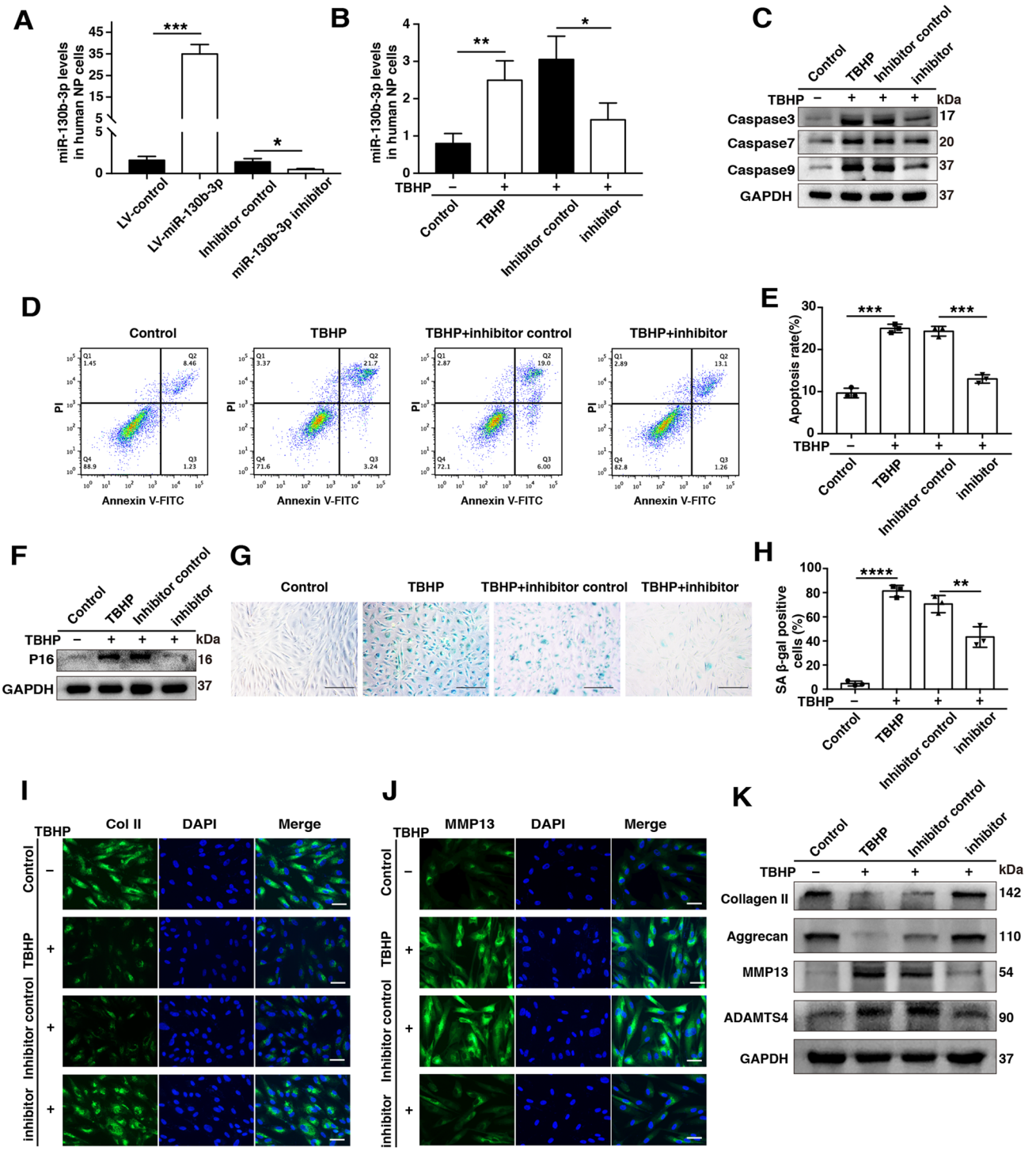

Fig. 2 Inhibition of miR-130b-3p rescues the oxidative stress-induced dysfunction of human NP cells. **A** Human NP cells were transfected with the LV-miR-130b-3p, miR-130b-3p inhibitor, and corresponding controls. The miR-130b-3p levels in human NP cells were analyzed by qRT-PCR. **B** Human NP cells were transfected with miR-130b-3p inhibitor and inhibitor controls and then treated with TBHP (100 μm). qRT-PCR was used to detect the miR-130b-3p level of all groups. **C** Western blot showed the level of Caspase3, Caspase7, and Caspase9 after treatment with the TBHP, miR-130b-3p inhibitor, or inhibitor controls. **D**, **E** The NP cells' apoptotic rate of each group as treated above was detected by flow cytometry. **F** Representative Western blots data of p16. **G**, **H** SA-β-gal staining assay was performed in human NP cells of each group (Scale bar, 200 μm). **I**, **J** The representative collagen II and MMP13 were detected by the immunofluorescence (Scale bars, 50 μm). **K** The protein levels of collagen II, aggrecan, MMP13, and ADAMTS4 were detected by Western blot. All data are presented as the mean ± SD. TBHP: Tert-butyl hydroperoxide. $^{*}P < 0.05$; $^{**}P < 0.01$; $^{***}P < 0.001$

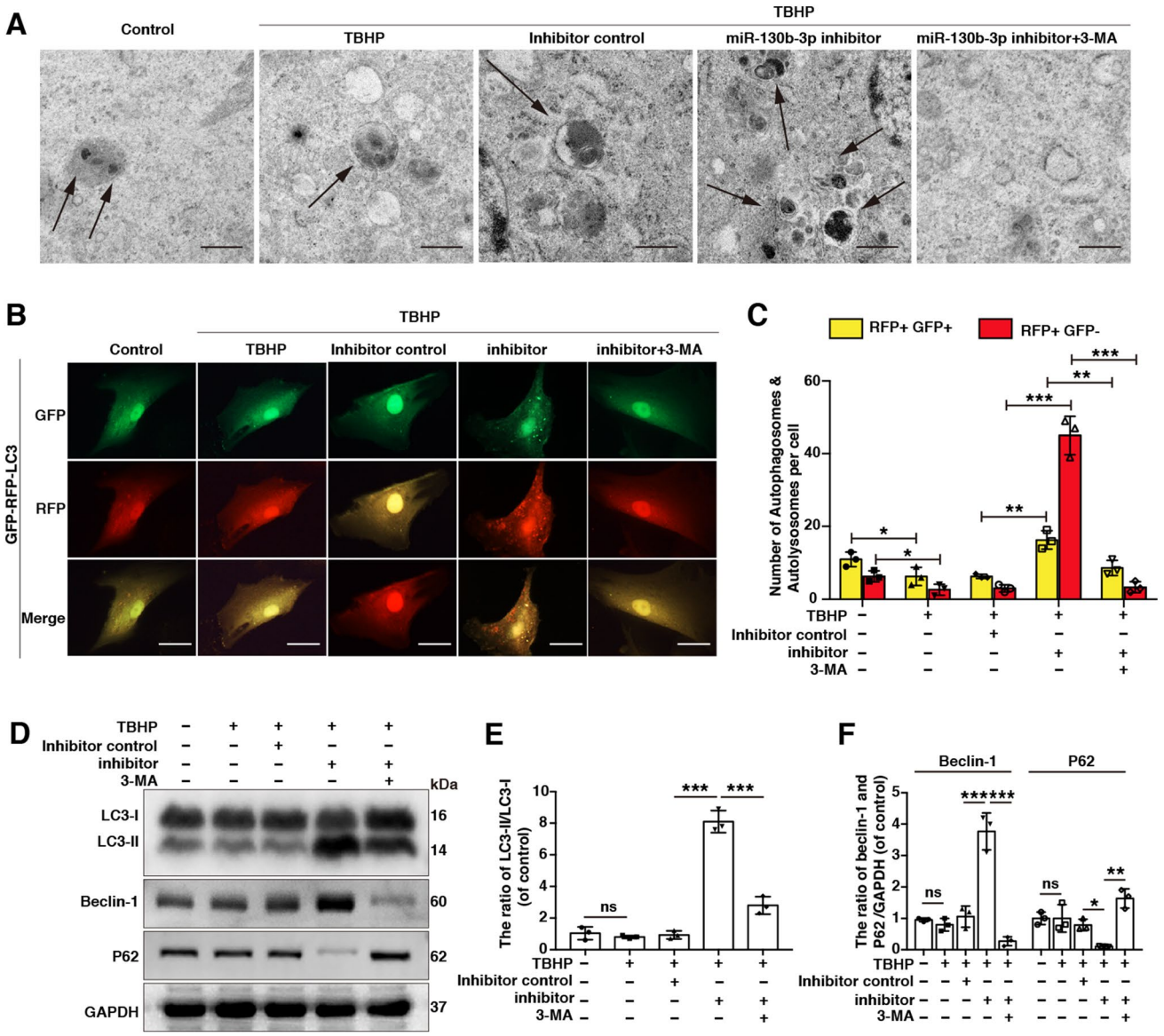

Fig. 3 The miR-130b-3p inhibition upregulated autophagy in human NP cells under oxidative stress. **A** Transmission electron microscopy showed the autophagosomes (black arrow: autophagosome) in human NP cells of all groups (Scale bars, 0.5 μm). **B**, **C** Human NP cells transfected with Ad-mRFP-GFP-LC3. Autophagosomes are labeled both with GFP and mRFP and appear yellow, whereas autolysosomes are labeled with mRFP only and appear red in the merged image (Scale bars, 25 μm). **D**–**F** Representative Western blots and quantification data of LC3, Beclin-1, and P62 protein in human NP cells of each group. 3-MA: 3-Methyladenine. All data are presented as the mean ± SD. *$P < 0.05$; **$P < 0.01$; ***$P < 0.001$

which might play a role in the pathological processes of the IVDD.

The ATG14 and PRKAA1 are direct target genes of the miR-130b-3p

The bioinformatic website of TargetScan (http://www.targetscan.org/) was used to predict the target genes of the miR-130b-3p. Notably, the ATG14 and PRKAA1, two autophagy-related genes, were identified as potential miR-130b-3p targets (Fig. 4A). To verify whether the ATG14 and PRKAA1 were direct targets of the miR-130b-3p, a dual-luciferase reporter system was used. We found that the miR-130b-3p overexpression significantly repressed the luciferase activity of both wild-type ATG14 and PRKAA1 3′-UTR whereas the mutant 3′-UTR was not affected in the HEK 293 cells [Fig. 4B, ($P < 0.01$)]. The Western blot revealed that compared with the control group, the miR-130b-3p overexpression greatly reduced the level of the ATG14 and PRKAA1 while

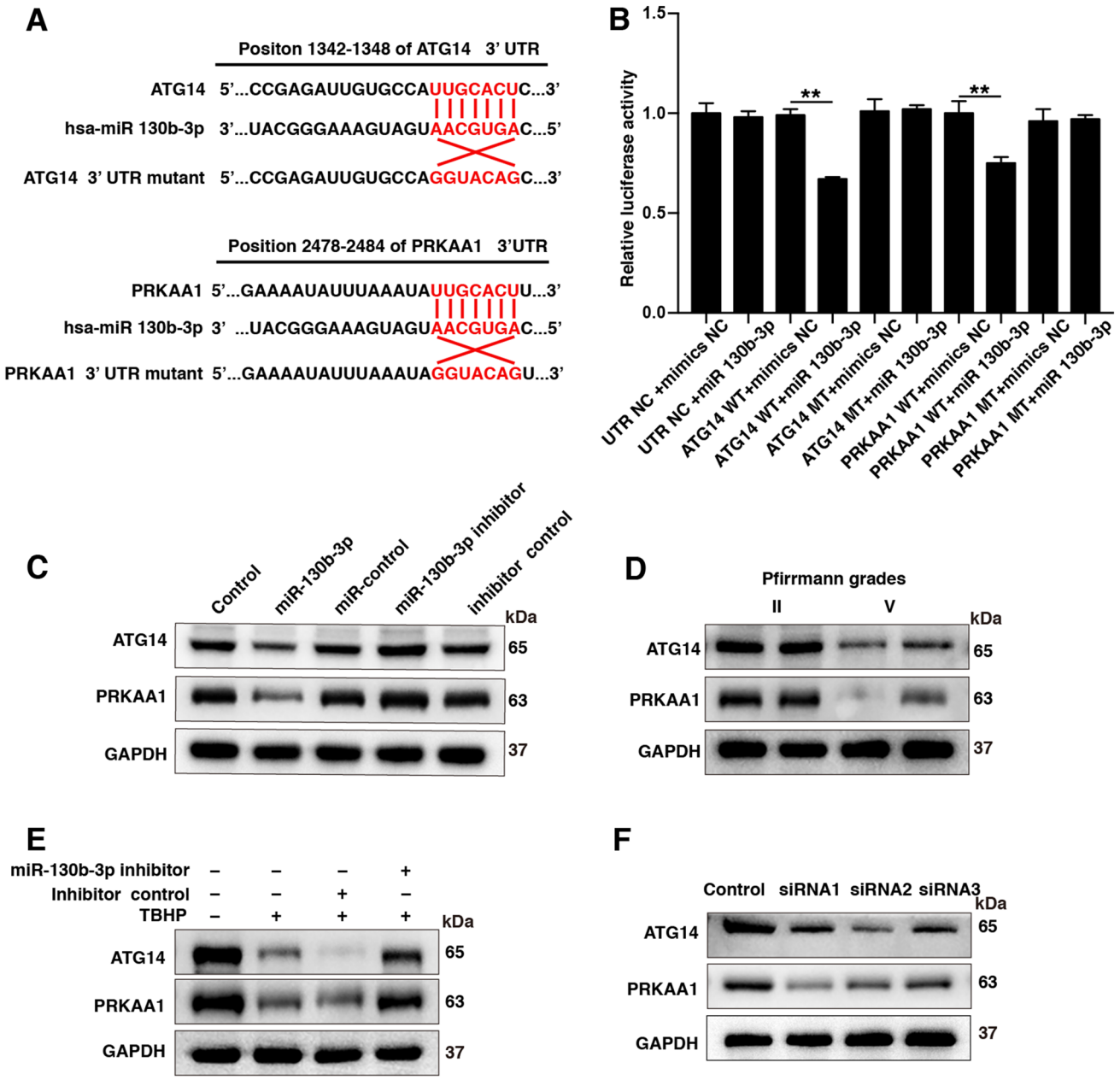

Fig. 4 ATG14 and PRKAA1 are direct target genes of miR-130b-3p. **A** The predictive target sequence for miR-130b-3p at the 3'UTR of ATG14 and PRKAA1. **B** Dual-luciferase assays were performed in HEK 293 cells after co-transfection with the wild-type or mutant ATG14 and PRKAA1 3' UTR plasmids and NC or miR-130b-3p mimics. **C** Human NP cells were transfected with miR-130b-3p, inhibitor or NC, and the expression of ATG14 and PRKAA1 was determined using Western blot analysis. **D** Western blot was used to determine the protein level of ATG14 and PRKAA1 in patients' NP tissue (Pfirrmann grades II and V). **E**, **F** Western blots showed the level of ATG14 and PRKAA1 after treatment with TBHP, miR-130b-3p inhibitor, or inhibitor controls and after a knockdown by siRNA. All data are presented as the mean ± SD. $^{*}P < 0.05$; $^{**}P < 0.01$; $^{***}P < 0.001$

the miR-130b-3p inhibition caused the opposite results (Fig. 4C). We observed that the ATG14 and PRKAA1 expression were downregulated in the severe degenerative human NP tissues (Pfirrmann grades V) compared with the mild degenerative ones (Pfirrmann grades II) (Fig. 4D). The TBHP treatment reduced the expression of the ATG14 and PRKAA1 in human NP cells, while the miR-130b-3p inhibition alleviated this reduction (Fig. 4E). To further explore whether the miR-130b-3p exerted its functions through targeting the ATG14 and PRKAA1 in the human NP cells, the ATG14 and PRKAA1 were knocked down by siRNA transfection. According to the knockdown efficiency, the siRNA2 of ATG14 and siRNA1 of PRKAA1 were chosen for further use (Fig. 4F).

The miR-130b-3p regulates autophagy by targeting the ATG14 and PRKAA1

Based on the above data, we hypothesized that the miR-130b-3p mediates autophagy through ATG14 and PRKAA1. To validate this hypothesis, we further co-transfected the human NP cells with the miR-130b-3p inhibitor and siRNAs targeting the ATG14 or PRKAA1. The TEM result indicated that the ATG14 and PRKAA1 knockdown could suppress the autophagy that was promoted by the miR-130b-3p inhibition in the TBHP-induced cells (Fig. 5A). Moreover, the AdV-mRFP-GFP-LC3 system data suggested that the number of both autophagosomes and autolysosomes were decreased after the ATG14 and PRKAA1 knockdown

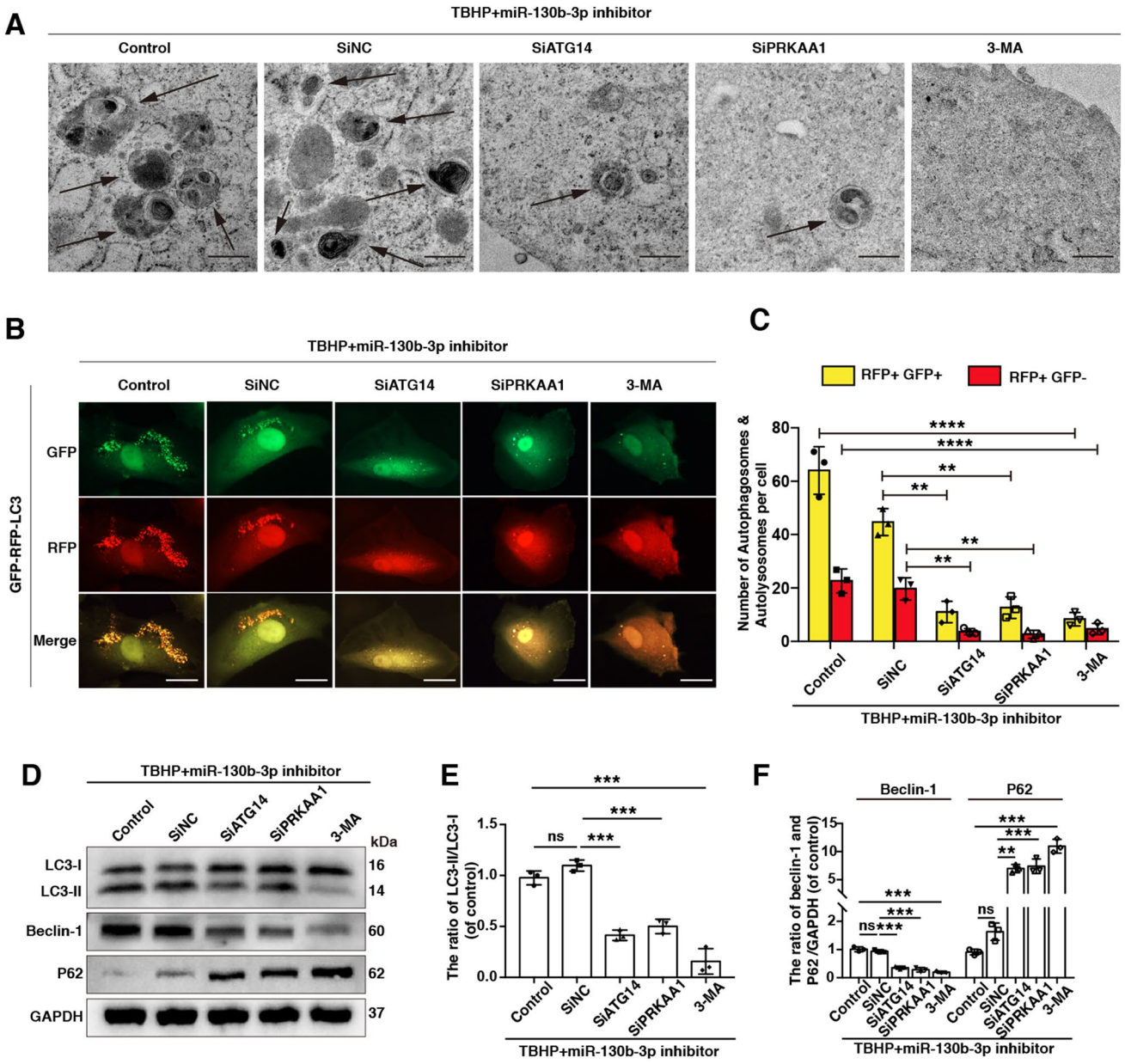

Fig. 5 The miR-130b-3p regulated autophagy by targeting ATG14 and PRKAA1. **A** Human NP cells were co-transfected with miR-130b-3p and ATG14 siRNA or PRKAA1 siRNA and then exposed to TBHP or 3-MA. Transmission electron microscopy showed the autophagosomes (black arrow, autophagosome) in the above all groups (Scale bars, 0.5 μm). **B**, **C** Representative images of LC3 staining by infecting human NP cells with RFP-GFP-LC3 adenovirus in all groups (Scale bar, 25 μm). **D**, **E**, **F** Representative Western blots and quantification data of LC3, Beclin-1, and P62 protein in human NP cells of each group. All data are presented as the mean ± SD. $^{*}P < 0.05$; $^{**}P < 0.01$; $^{***}P < 0.001$

although the miR-130b-3p expression was inhibited [Fig. 5B, C, ($P < 0.01$)]. Finally, the ATG14 and PRKAA1 knockdown repressed the protein level of the LC3-II and Beclin-1 while enhanced the P62 expression in the miR-130b-3p inhibited human NP cells, which also implied the reduced autophagy level [Fig. 5D–F, ($P < 0.01$)]. These results validated that the miR-130b-3p mediated the autophagy by targeting the ATG14 and PRKAA1.

Inhibition of miR-130b-3p rescued the dysfunction of human NP cells through regulating the autophagy-related genes ATG14 and PRKAA1

The human NP cells were co-transfected with the miR-130b-3p inhibitor and siATG14 or siPRKAA1. Firstly, the flow cytometry and Western blot results showed that the ATG14 and PRKAA1 knockdown enhanced the apoptotic rate that was ever restrained when the miR-130b-3p expression was inhibited in the TBHP-induced cells [Fig. 6A–C, ($P < 0.05$)]. Next, the downregulation of the ATG14 and PRKAA1 counteracted the anti-senescence effect of the miR-130b-3p inhibition in the human NP cells [Fig. 6D–F, ($P < 0.001$)]. Moreover, the catabolic effects of the TBHP in the cells were promoted, and the level of collagen II and aggrecan was repressed in the absence of the ATG14 and PRKAA1 (Fig. 6G–I). Our data have demonstrated that the 3-MA could robustly block the autophagic flux. In this study, we observed that the protective effects of the miR-130b-3p inhibition were abolished when the 3-MA was used in the human NP cells. Collectively, these data suggested that the miR-130b-3p function in the human NP cells was autophagy-dependent and through modulating the ATG14 and PRKAA1.

Inhibition of the miR-130b-3p rescues the IVDD in a rat model

The rats were randomly divided into four groups (Control, IVDD, miR-130b-3p inhibitor, and Inhibitor control). To investigate the therapeutic role of the miR-130b-3p in IVDD, a rat model of the IVDD was successfully constructed via needle puncture, and then a total of 3 μL HBAAV2/9-rno-Mir-130b-3p-sponge-EGFP or HBAAV2/9-EGFP NC were intradiscally injected using a 27 G needle. The effective transfection efficiency of the HBAAV2/9 in the injected rat discs was observed by the immunofluorescence two weeks after transfection (Supplemental Fig. 1). The MRI examination was performed at times 0, 4, and 8 weeks in all groups. As shown in Fig. 7A, B, at 4 and 8 weeks after surgery, the Pfirrmann grades of the rat intervertebral discs were remarkably higher in the IVDD group than the control group whereas the miR-130b-3p inhibition could significantly decrease the degenerative degree score ($P < 0.05$). After the MRI scanning, all rats were sacrificed and pathological staining including HE and SO was carried out. The histological scores of the rat discs in the IVDD group were higher than those in the control group while the miR-130b-3p inhibition obtained lower histological scores than the inhibitor control group [Fig. 7C, D; Supplemental Fig. 2, ($P < 0.01$)]. Interestingly, as documented by the immunofluorescence staining, the protein expression of the LC3, ATG14, PRKAA1, and collagen II were increased in the miR-130b-3p knockdown NP tissues in vivo, compared with the inhibitor control group (Fig. 8A–D). These results indicated that the knockdown of miR-130b-3p could stimulate autophagy and ameliorate the IVDD in vivo (Fig. 9).

Discussion

The IVDD is the main risk factor leading to LBP, which causes a huge healthcare burden worldwide every year [33]. Despite the considerable development of medicine, the clinical treatment of IVDD remains limited. Therefore, a better understanding of the pathogenesis of the IVDD and effective therapies are presently needed. A previous study reported that the senescence, apoptosis, and aberrant ECM metabolism of the NP cells are the key characteristic of the IVDD [34]. Although many factors could accelerate the degeneration of the intervertebral disc, severe oxidative stress is considered critical. Apart from inducing senescence and apoptosis of the NP cells, oxidative stress could negatively regulate the production of ECM and the high levels of oxidative stress are correlated with severe disc degeneration. However, the pathological mechanism of this connection is still unclear. In order to explore the pathogenetic mechanism of oxidative stress in the IVDD, in our research, the human NP cells were treated with 100 μM TBHP for 24 h. We observed that the percentage of senescence and apoptosis was increased along with the imbalance of the ECM metabolism in the human NP cells after the stimulation by the TBHP, which indicated that oxidative stress led to the NP cells' degeneration.

Autophagy plays an exceptional role in cell survival, during which the cytoplasmic proteins or organelles are phagocytosed into vesicles and fused with the lysosomes to form autophagolysosomes and degrade their encapsulated contents [30]. Oxidative stress could affect autophagy in many diseases such as cancer, diabetes, and neurodegenerative diseases [35–37]. Accumulating evidence demonstrated that autophagy was related to the oxidative stress level of IVDD [6, 38]. Some scholars reported that excessive oxidative stress blocks the autophagic flux in the degenerative disc whereas a moderate level of oxidative stress promoted autophagy, which exerted a protective effect on the NP cells [39, 40]. Some studies revealed that compared

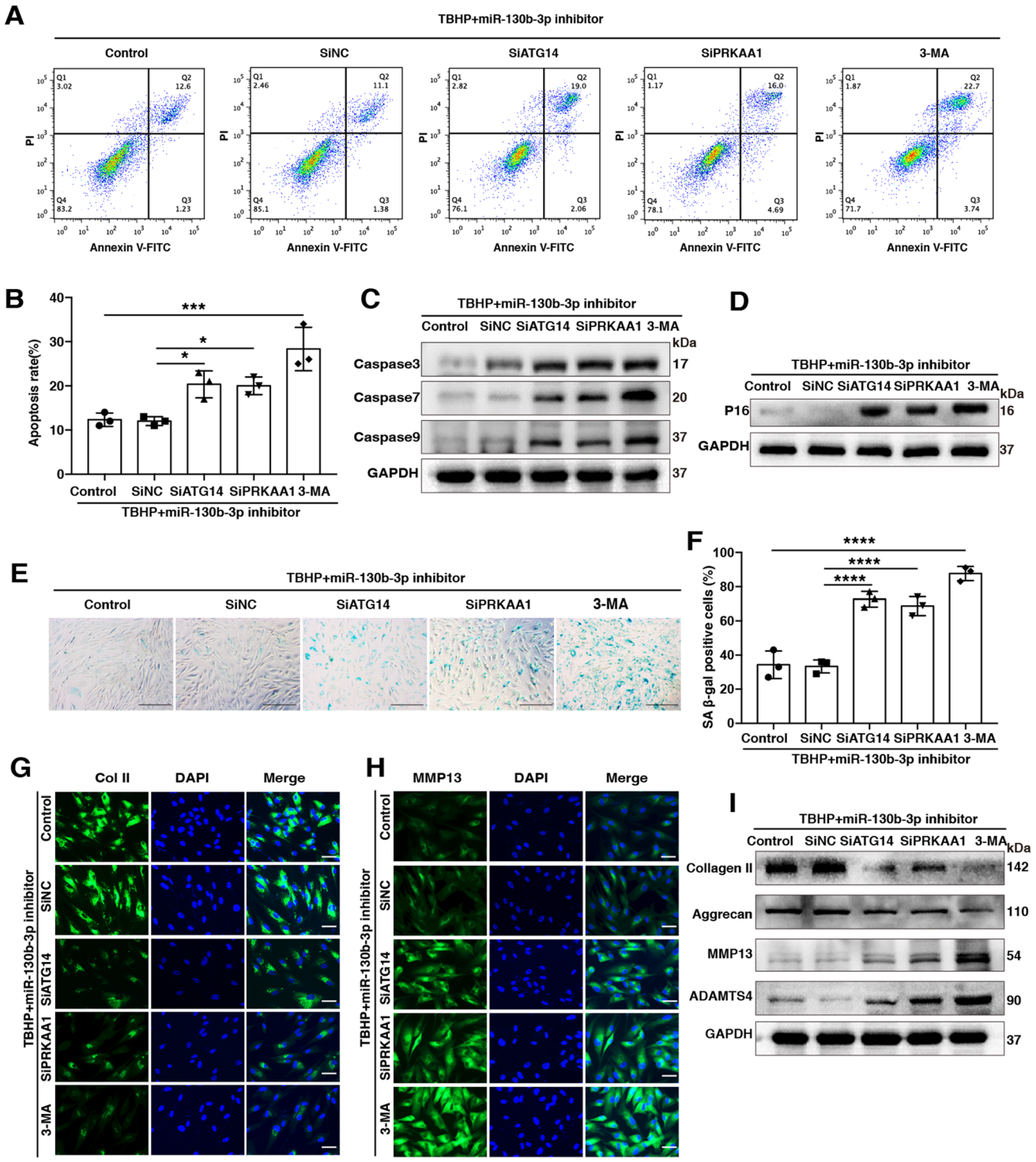

Fig. 6 Inhibition of miR-130b-3p rescued the dysfunction of human NP cells through regulating autophagy-related genes ATG14 and PRKAA1. **A**–**C** The human NP cells apoptotic rate of each group as treated above was detected by flow cytometry and Western blot was used to determine the level Caspase3, Caspase7, and Caspase9. **D–F** The senescence of cells of all groups was revealed by SA-β-gal staining and the p16 protein level was detected by Western blot (Scale bar, 200 μm). **G**–I Immunofluorescence showed the protein level of collagen II and MMP13 in each group (Scale bars, 50 μm). And the protein levels of collagen II, aggrecan, MMP13, and ADAMTS4 were detected by Western blot. All data are presented as the mean ± SD. $^{*}P < 0.05$; $^{**}P < 0.01$; $^{***}P < 0.001$

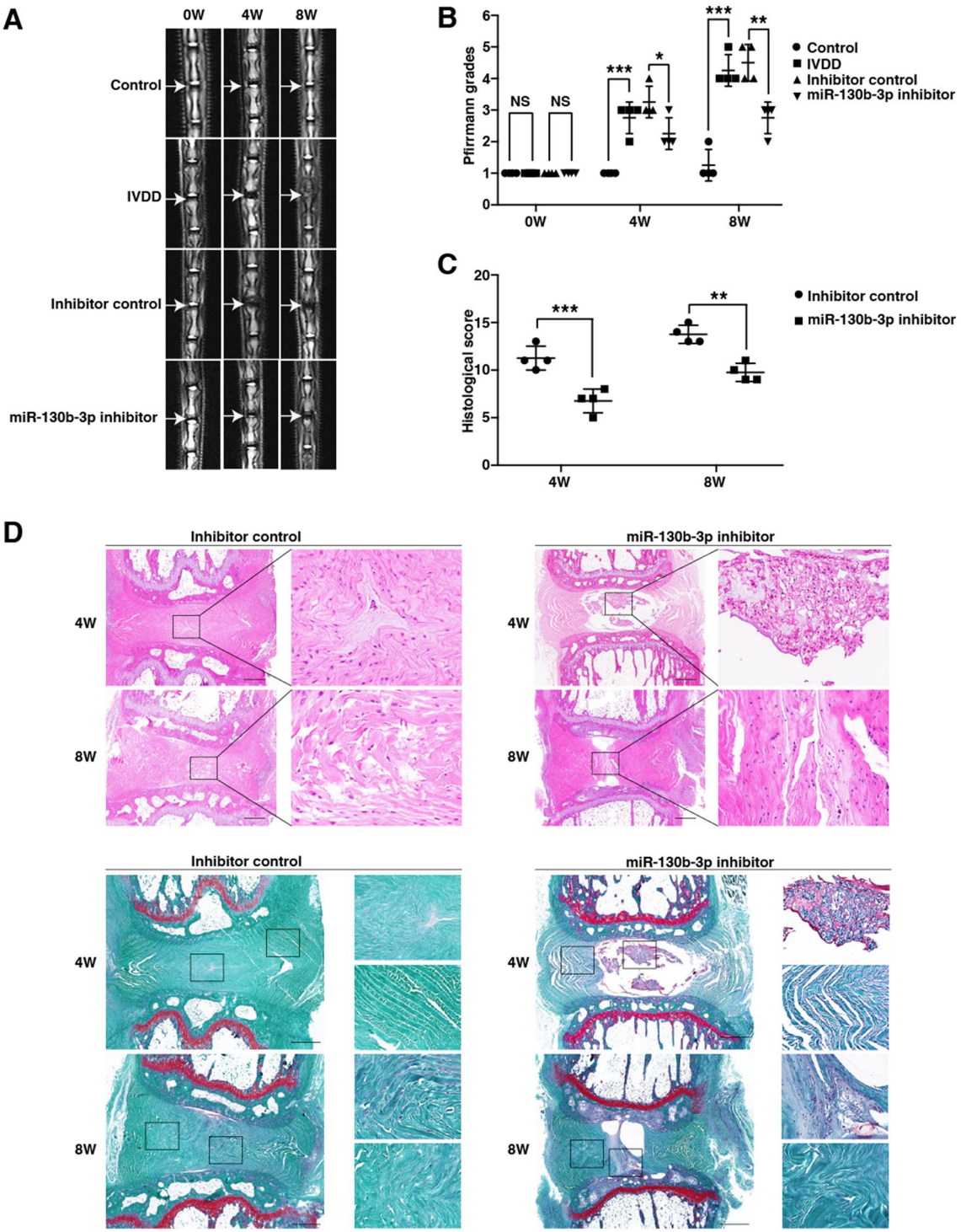

Fig. 7 Inhibition of miR-130b-3p rescued the IVDD in a rat model. **A** T2-weighted MRI of a rat-tail disc at 0, 4, and 8 weeks after needle puncture (white arrows). **B** Respective Pfirrmann grades of each group at 0, 4, and 8 weeks after needle puncture. **C**, **D** Hematoxylin–eosin (HE) and safranin-O/fast green staining of the intervertebral discs in the miR-130b-3p inhibitor and control groups at 4 and 8 weeks after injection. And then the histological score was evaluated in the two groups (Scale bar, 500 μm). n = 4. All data are presented as the mean ± SD. $^{*}P < 0.05$; $^{**}P < 0.01$; $^{***}P < 0.001$

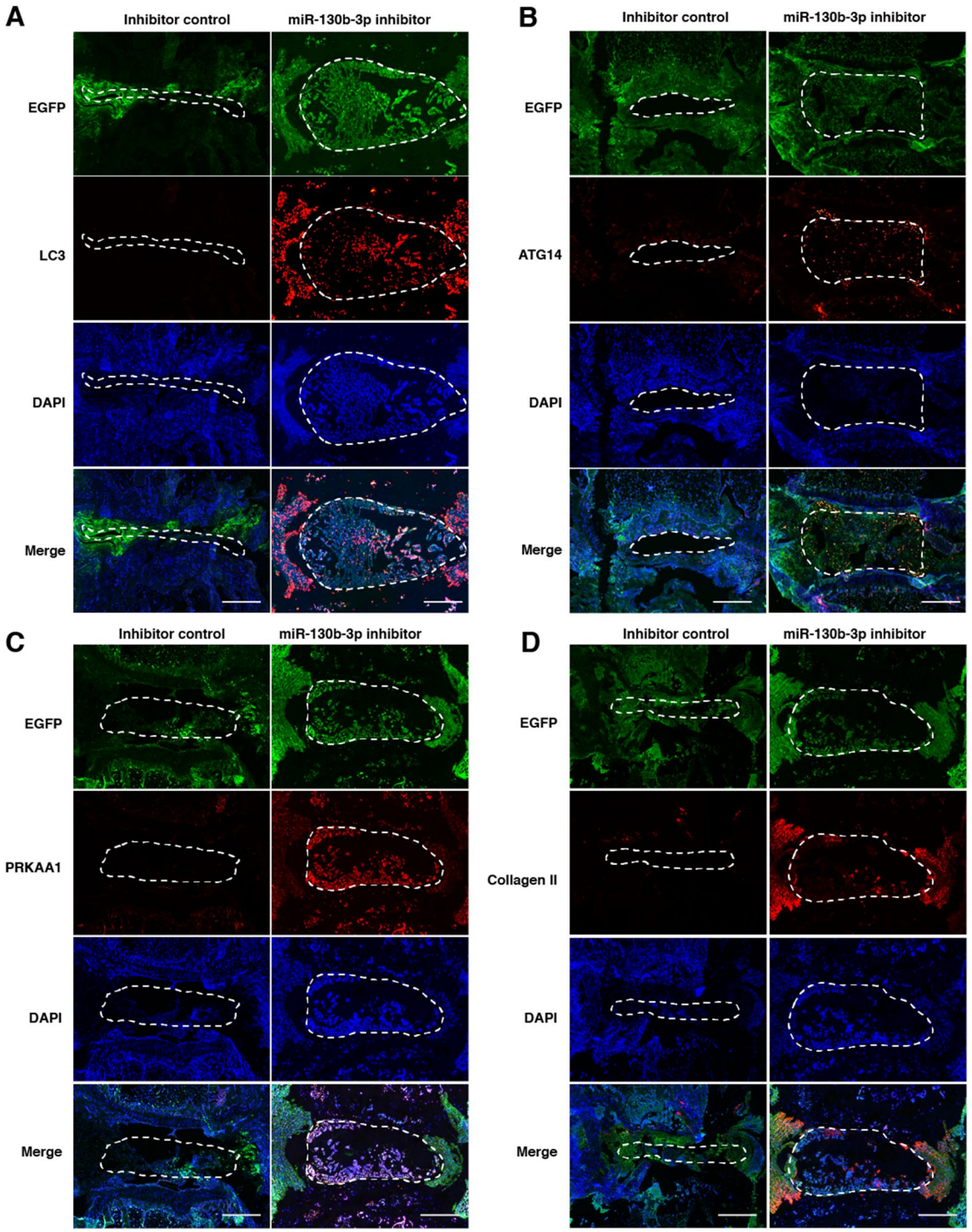

Fig. 8 The protein level of LC3, ATG14, PRKAA1, and collagen II were escalated in miR-130b-3p knockdown NP in vivo. **A**–**D** The double immunofluorescence staining of EGFP and LC3, ATG14, PRKAA1, or collagen II in NP tissues from different groups at 4 weeks post-surgery (Scale bar, 500 μm). n = 4. EGFP, green; LC3, ATG14, PRKAA1, or collagen II, red; DAPI, blue. White lines marked areas: nucleus pulposus tissues

with the nondegenerative NP cells, more autophagic flux was observed in the degenerative NP cells. The other studies demonstrated that autophagy was inhibited in the degenerated NP cells of rats [15, 41, 42]. In our research, we found that the THBP induced oxidative stress could suppress the autophagic flux, though the protein levels of

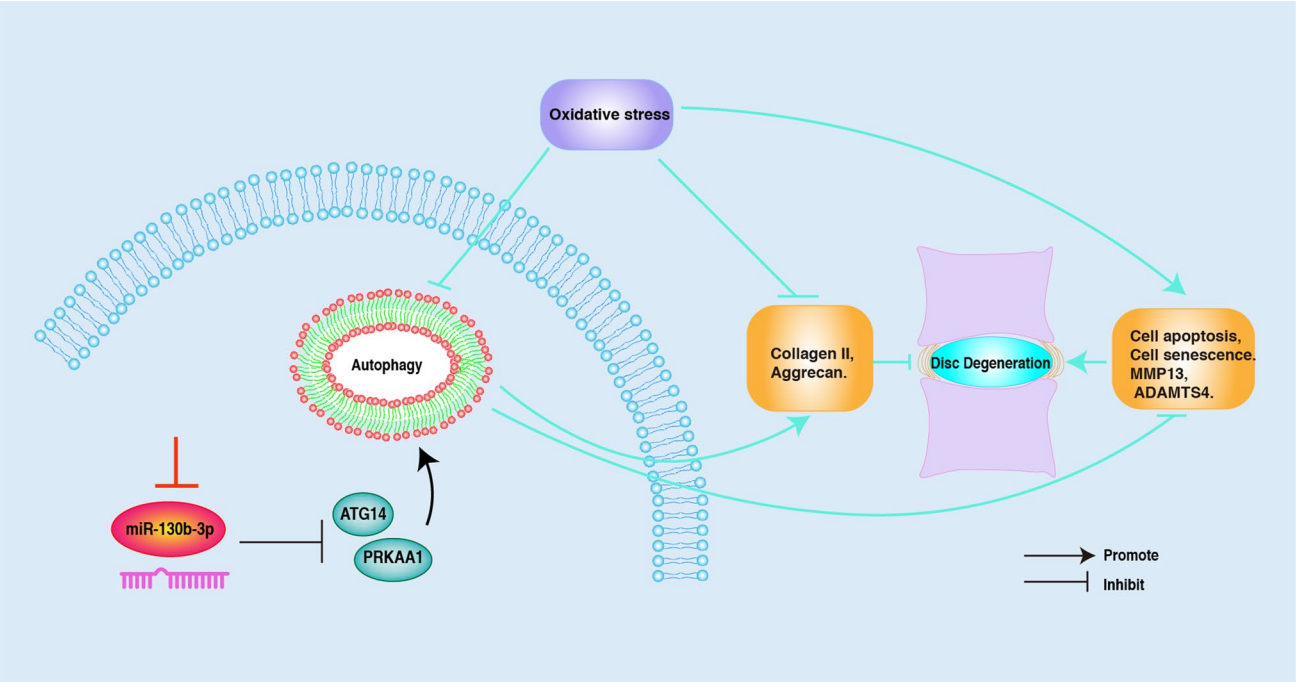

Fig. 9 Schematic diagram of the protective effects of miR-130b-3p inhibition on IVDD. Under the circumstance of oxidative stress, miR-130b-3p inhibition restored autophagy via ATG14 and PRKAA1 in NP, leading to suppression of cell apoptosis and senescence, decreased level of MMP13 and ADAMTS4, and increased collagen II and aggrecan levels

LC3A/B, Beclin-1, and p62 have not been changed greatly. In our opinion, excessive oxidative stress will blockade the autophagic flux in the NP cells, which eventually facilitates the development of the IVDD. But the effect of oxidative stress on autophagy in the process of IVDD remains to be determined.

miRNAs are a class of non-coding RNAs that negatively regulate the target gene expression post-transcriptionally. It was reported that the miRNAs played an important role in multiple physiological and pathological processes since the discovery of miRNAs [43]. Among miRNAs, miR-130b has been reported to function as an oncogene in various cancers [20]. In addition, previous studies reported that the inhibition of miR-130b-3p exerted a protective effect on the placental trophoblast cells against oxidative stress [21]. In our study, we aimed to investigate whether the miR-130b-3p was involved in the IVDD and its regulation of the autophagy mechanism.

Through the qRT-PCR and FISH assay, we found that the miR-130b-3p was upregulated in the degenerative NP samples of humans and rats. Besides, the miR-130b-3p expression was positively correlated with the Pfirrmann grades of the IVDD patients. These results indicated the potential role of the miR-130b-3p in the IVDD. Stable knocked down or overexpression of the miR-130b-3p in the human NP cells was constructed via the lentivirus transfection. To mimic the IVDD in vitro, the human NP cells were treated with the TBHP (100 μM) for 24 h to induce oxidative stress [44]. Herein, we demonstrated that the miR-130b-3p knockdown could suppress the apoptosis and senescence as well as improve the ECM metabolism of human NP cells after the TBHP treatment. These data implied that the miR-130b-3p inhibition could protect the human NP cells from oxidative stress-induced dysfunction. It was reported that the autophagy was related to the IVDD and we found that the miR-130b-3p could directly regulate the autophagy-related genes ATG14 or PRKAA1 predicted via bioinformatics and luciferase assay [32]. The ATG14, also known as beclin-1-associated autophagy-related key regulator (Barkor or ATG14L), played an essential role in facilitating the membrane tethering and fusion of autophagosomes to endolysosomes during autophagy [22, 45]. The PRKAA1 (protein kinase AMP-activated catalytic subunit alpha 1) was reported to mediate autophagy in multiple diseases, including leukemia, wound healing, and osteoarthritis [23–25]. However, it was unclear whether the miR-130b-3p could regulate the autophagy in the IVDD via mediating its target genes. To answer this question, we detected the autophagy level under the conditions of miR-130b-3p inhibition. Autophagy was monitored via the TEM, AdV-mRFP-GFP-LC3 system, and Western blot [30]. Interestingly, the miR-130b-3p inhibition could upregulate autophagy in the TBHP-treated human NP cells. But, compared with the control

group, the knockdown of ATG14 or PRKAA1 and the treatment of autophagy inhibitor (3-MA) significantly suppressed the autophagic flux in the miR-130b-3p inhibition group, which implied that the miR-130b-3p regulation on autophagy depended on the ATG14 and PRKAA1. Furthermore, with the knockdown of ATG14 or PRKAA1 or the treatment of 3-MA, the anti-degeneration role of the miR-130b-3p inhibition in the human NP cells was blocked. Finally, in the in vivo experiment, the AAV-miR-130b-3p inhibitor and its control were injected into the rat coccygeal disc. Through the MRI scanning and histological staining, we observed that inhibition of miR-130b-3p could ameliorate the IVDD in a rat model.

However, there were some limitations involved in our research. First, we only found that the miR-130b-3p alleviated the IVDD via regulating autophagy. It is not clear whether the miR-130b-3p exerts its role in other ways. More studies need to be carried out to elucidate the protective effects of the miR-130b-3p in the IVDD. Second, to further support the conclusion of animal experiments, the sample size needs to be increased in the in vivo experiments in the future.

In conclusion, we revealed that the miR-130b-3p was dysregulated in the IVDD and the miR-130b-3p inhibition could alleviate the IVDD via anti-apoptosis, antisenescence, and improvement of the metabolism in the human NP cells. Mechanistically, we found that the miR-130b-3p exerts its protective role by regulating autophagy. Therefore, our research demonstrated that the miR-130b-3p may be an effective therapeutic target in the treatment of IVDD.

Supplementary Information The online version contains supplementary material available at https://doi.org/10.1007/s10495-022-01725-0.

Acknowledgements We would like to thank all members of the laboratory for suggestions and technical supports.

Author contributions DW and TW conceptualized the study; TW wrote the primary manuscript; XJ, KG, ZZ were responsible for revising the manuscript and collecting the data. DW, QW, ZG, and XL analyzed the data. TW, XJ, and KG performed the experiments. YH and DW provided funding for this research.

Funding Our research was supported by National Natural Science Foundation of China (No. 81972106), Shanghai Natural Science Foundation (No. 19ZR1441700; Shanghai, China), and Discipline Leader Training Project of Pudong New Area Municipal Health Commission (No. PWRd2020-03; Shanghai, China).

Declarations

Conflict of interest The authors declare no competing financial interests.

Consent for publication The authors have reviewed the final version of the manuscript and approve it for publication.

Ethical approval The patients' samples collection was approved by the Ethics Committee of the Shanghai East Hospital. The informed consent form was signed by the patients before collecting the samples. The animal use and care protocols were approved by the Shanghai East Hospital Animal Care and Use Committee.

Availability of data and materials All data used and analyzed during the current study are available from the corresponding author on reasonable request.

References

1. Ropper AH, Zafonte RD (2015) Sciatica. N Engl J Med 372(13):1240–1248
2. Ali R et al (2016) Global, regional, and national incidence, prevalence, and years lived with disability for 310 diseases and injuries, 1990–2015: a systematic analysis for the Global Burden of Disease Study 2015. Lancet 388(10053):1545–602
3. Cheng X, Zhang L, Zhang K, Zhang G, Hu Y, Sun X et al (2018) Circular RNA VMA21 protects against intervertebral disc degeneration through targeting miR-200c and X linked inhibitor-of-apoptosis protein. Ann Rheum Dis 77(5):770–779
4. Ji ML, Jiang H, Zhang XJ, Shi PL, Li C, Wu H et al (2018) Preclinical development of a microRNA-based therapy for intervertebral disc degeneration. Nat Commun 9(1):5051
5. Freemont AJ, Watkins A, Le Maitre C, Jeziorska M, Hoyland JA (2002) Current understanding of cellular and molecular events in intervertebral disc degeneration: implications for therapy. J Pathol 196(4):374–379
6. Chen D, Xia D, Pan Z, Xu D, Zhou Y, Wu Y, et al. Metformin protects against apoptosis and senescence in nucleus pulposus cells and ameliorates disc degeneration in vivo. Cell Death Dis 2016;7(10):e2441.
7. Che H, Li J, Li Y, Ma C, Liu H, Qin J et al (2020) p16 deficiency attenuates intervertebral disc degeneration by adjusting oxidative stress and nucleus pulposus cell cycle. Elife 20:9. https://doi.org/10.7554/eLife.52570
8. Battié MC, Videman T, Parent E (2004) Lumbar disc degeneration: epidemiology and genetic influences. Spine (Phila Pa 1976) 29(23):2679–90
9. Nakamichi R, Ito Y, Inui M, Onizuka N, Kayama T, Kataoka K et al (2016) Mohawk promotes the maintenance and regeneration of the outer annulus fibrosus of intervertebral discs. Nat Commun 7:12503
10. Mariño G, Niso-Santano M, Baehrecke EH, Kroemer G (2014) Self-consumption: the interplay of autophagy and apoptosis. Nat Rev Mol Cell Biol 15(2):81–94
11. Chen C, Yang S, Li H, Yin Z, Fan J, Zhao Y et al (2017) Mir30c is involved in diabetic cardiomyopathy through regulation of cardiac autophagy via BECN1. Mol Ther Nucleic Acids 7:127–139
12. Fang EF, Hou Y, Palikaras K, Adriaanse BA, Kerr JS, Yang B et al (2019) Mitophagy inhibits amyloid-β and tau pathology and reverses cognitive deficits in models of Alzheimer's disease. Nat Neurosci 22(3):401–412
13. Matsuzaki T, Alvarez-Garcia O, Mokuda S, Nagira K, Olmer M, Gamini R et al (2018) FoxO transcription factors modulate autophagy and proteoglycan 4 in cartilage homeostasis and osteoarthritis. Sci Transl Med. https://doi.org/10.1126/scitranslmed.aan0746
14. Tang Z, Hu B, Zang F, Wang J, Zhang X, Chen H (2019) Nrf2 drives oxidative stress-induced autophagy in nucleus pulposus cells via a Keap1/Nrf2/p62 feedback loop to protect intervertebral disc from degeneration. Cell Death Dis 10(7):510

15. Chen Y, Lin J, Chen J, Huang C, Zhang Z, Wang J et al (2020) Mfn2 is involved in intervertebral disc degeneration through autophagy modulation. Osteoarthritis Cartilage 28(3):363–374
16. Bartel DP (2009) MicroRNAs: target recognition and regulatory functions. Cell 136(2):215–233
17. Wang WJ, Yang W, Ouyang ZH, Xue JB, Li XL, Zhang J et al (2018) MiR-21 promotes ECM degradation through inhibiting autophagy via the PTEN/akt/mTOR signaling pathway in human degenerated NP cells. Biomed Pharmacother 99:725–734
18. Wang C, Zhang ZZ, Yang W, Ouyang ZH, Xue JB, Li XL et al (2017) MiR-210 facilitates ECM degradation by suppressing autophagy via silencing of ATG7 in human degenerated NP cells. Biomed Pharmacother 93:470–479
19. Mao Z, Yao M, Li Y, Fu Z, Li S, Zhang L et al (2018) miR-96-5p and miR-101-3p as potential intervention targets to rescue TiO(2) NP-induced autophagy and migration impairment of human trophoblastic cells. Biomater Sci 6(12):3273–3283
20. Kim Y, Kim H, Bang S, Jee S, Jang K (2021) MicroRNA-130b functions as an oncogene and is a predictive marker of poor prognosis in lung adenocarcinoma. Lab Invest 101(2):155–164
21. Jiang S, Teague AM, Tryggestad JB, Chernausek SD (2017) Role of microRNA-130b in placental PGC-1α/TFAM mitochondrial biogenesis pathway. Biochem Biophys Res Commun 487(3):607–612
22. Diao J, Liu R, Rong Y, Zhao M, Zhang J, Lai Y et al (2015) ATG14 promotes membrane tethering and fusion of autophagosomes to endolysosomes. Nature 520(7548):563–566
23. Yang H, Wen Y, Zhang M, Liu Q, Zhang H, Zhang J et al (2020) MTORC1 coordinates the autophagy and apoptosis signaling in articular chondrocytes in osteoarthritic temporomandibular joint. Autophagy 16(2):271–288
24. Qiang L, Yang S, Cui YH, He YY (2020) Keratinocyte autophagy enables the activation of keratinocytes and fibroblasts and facilitates wound healing. Autophagy 17:2128–2143
25. Obba S, Hizir Z, Boyer L, Selimoglu-Buet D, Pfeifer A, Michel G et al (2015) The PRKAA1/AMPKα1 pathway triggers autophagy during CSF1-induced human monocyte differentiation and is a potential target in CMML. Autophagy 11(7):1114–1129
26. Wu T, Li X, Jia X, Zhu Z, Lu J, Feng H et al (2021) Krüppel like factor 10 prevents intervertebral disc degeneration via TGF-β signaling pathway both in vitro and in vivo. J Orthop Translat 29:19–29
27. Pfirrmann CW, Metzdorf A, Zanetti M, Hodler J, Boos N (2001) Magnetic resonance classification of lumbar intervertebral disc degeneration. Spine (Phila Pa 1976) 26(17):1873–1878
28. Guo J, Shao M, Lu F, Jiang J, Xia X (2017) Role of Sirt1 plays in nucleus pulposus cells and intervertebral disc degeneration. Spine (Phila Pa 1976) 42(13):e757–e766
29. Wu T, Jia X, Feng H, Wu D (2021) ACTG1 regulates intervertebral disc degeneration via the NF-κB-p65 and Akt pathways. Biochem Biophys Res Commun 545:54–61
30. Klionsky DJ, Abdelmohsen K, Abe A, Abedin MJ, Abeliovich H, Acevedo Arozena A et al (2016) Guidelines for the use and interpretation of assays for monitoring autophagy (3rd edition). Autophagy 12(1):1–222
31. Zheng G, Pan Z, Zhan Y, Tang Q, Zheng F, Zhou Y et al (2019) TFEB protects nucleus pulposus cells against apoptosis and senescence via restoring autophagic flux. Osteoarthritis Cartilage 27(2):347–357
32. Sun K, Jing X, Guo J, Yao X, Guo F (2020) Mitophagy in degenerative joint diseases. Autophagy. https://doi.org/10.1080/15548627.2020.1822097
33. PUBMED CENTRAL (2015) Global, regional, and national incidence, prevalence, and years lived with disability for 301 acute and chronic diseases and injuries in 188 countries, 1990–2013: a systematic analysis for the Global Burden of Disease Study 2013. Lancet 386(9995):743–800
34. Guo Q, Zhu D, Wang Y, Miao Z, Chen Z, Lin Z et al (2021) Targeting STING attenuates ROS induced intervertebral disc degeneration. Osteoarthritis Cartilage 29(8):1213–1224
35. Komatsu M, Kurokawa H, Waguri S, Taguchi K, Kobayashi A, Ichimura Y et al (2010) The selective autophagy substrate p62 activates the stress responsive transcription factor Nrf2 through inactivation of Keap1. Nat Cell Biol 12(3):213–223
36. He C, Zhu H, Li H, Zou MH, Xie Z (2013) Dissociation of Bcl-2-Beclin1 complex by activated AMPK enhances cardiac autophagy and protects against cardiomyocyte apoptosis in diabetes. Diabetes 62(4):1270–1281
37. Menzies FM, Fleming A, Caricasole A, Bento CF, Andrews SP, Ashkenazi A et al (2017) Autophagy and neurodegeneration: pathogenic mechanisms and therapeutic opportunities. Neuron 93(5):1015–1034
38. Miyazaki S, Kakutani K, Yurube T, Maeno K, Takada T, Zhang Z et al (2015) Recombinant human SIRT1 protects against nutrient deprivation-induced mitochondrial apoptosis through autophagy induction in human intervertebral disc nucleus pulposus cells. Arthritis Res Ther 17(1):253
39. Chen JW, Ni BB, Li B, Yang YH, Jiang SD, Jiang LS (2014) The responses of autophagy and apoptosis to oxidative stress in nucleus pulposus cells: implications for disc degeneration. Cell Physiol Biochem 34(4):1175–1189
40. Chen JW, Ni BB, Zheng XF, Li B, Jiang SD, Jiang LS (2015) Hypoxia facilitates the survival of nucleus pulposus cells in serum deprivation by down-regulating excessive autophagy through restricting ROS generation. Int J Biochem Cell Biol 59:1–10
41. Ye W, Xu K, Huang D, Liang A, Peng Y, Zhu W et al (2011) Age-related increases of macroautophagy and chaperone-mediated autophagy in rat nucleus pulposus. Connect Tissue Res 52(6):472–478
42. Tang Q, Zheng G, Feng Z, Chen Y, Lou Y, Wang C et al (2017) Trehalose ameliorates oxidative stress-mediated mitochondrial dysfunction and ER stress via selective autophagy stimulation and autophagic flux restoration in osteoarthritis development. Cell Death Dis 8(10):e3081
43. Krol J, Loedige I, Filipowicz W (2010) The widespread regulation of microRNA biogenesis, function and decay. Nat Rev Genet 11(9):597–610
44. Xie L, Huang W, Fang Z, Ding F, Zou F, Ma X et al (2019) CircERCC2 ameliorated intervertebral disc degeneration by regulating mitophagy and apoptosis through miR-182-5p/SIRT1 axis. Cell Death Dis 10(10):751
45. Sun Q, Fan W, Chen K, Ding X, Chen S, Zhong Q (2008) Identification of Barkor as a mammalian autophagy-specific factor for Beclin 1 and class III phosphatidylinositol 3-kinase. Proc Natl Acad Sci U S A 105(49):19211–19216